In-beam γ-ray spectroscopy of ^{62,64}Cr

A. Gade,[1,2] R. V. F. Janssens,[3,4] D. Bazin,[1,2] P. Farris,[1,2] A. M. Hill,[1,2] S. M. Lenzi,[5] J. Li,[1] D. Little,[3,4] B. Longfellow,[1,2,*] F. Nowacki,[6,7] A. Poves,[8] D. Rhodes,[1,2] J. A. Tostevin,[9] and D. Weisshaar[1]

[1]*National Superconducting Cyclotron Laboratory, Michigan State University, East Lansing, Michigan 48824, USA*
[2]*Department of Physics and Astronomy, Michigan State University, East Lansing, Michigan 48824, USA*
[3]*Department of Physics and Astronomy, University of North Carolina at Chapel Hill, Chapel Hill, North Carolina 27599, USA*
[4]*Triangle Universities Nuclear Laboratory, Duke University, Durham, North Carolina 27708, USA*
[5]*Dipartimento di Fisica e Astronomia dell'Università and INFN, Sezione di Padova, I-35131 Padova, Italy*
[6]*Université de Strasbourg, IPHC, 23 Rue du Loess 67037 Strasbourg, France*
[7]*CNRS, UMR7178, 67037 Strasbourg, France*
[8]*Departamento de Física Teórica e IFT-UAM/CSIC, Universidad Autónoma de Madrid, E-28049 Madrid, Spain*
[9]*Department of Physics, Faculty of Engineering and Physical Sciences, University of Surrey, Guildford, Surrey GU2 7XH, United Kingdom*

(Received 8 September 2020; accepted 11 January 2021; published 20 January 2021)

The region of neutron-rich Cr isotopes has garnered much attention in recent years due to a rapid onset of collectivity near neutron number $N = 40$. We report here on the first γ-ray spectroscopy beyond the (4_1^+) state in ^{62,64}Cr, using nucleon removal reactions from several projectiles within a rare-isotope beam cocktail. A candidate for the 6^+ state in ^{64}Cr is presented as well as one for, possibly, the second excited 0^+ state in ^{62}Cr. The results are discussed in comparison to the LNPS shell-model predictions that allow for neutron excitations across the $N = 40$ harmonic oscillator gap into the $g_{9/2}$ and $d_{5/2}$ orbitals. The calculated level schemes for ^{62,64}Cr reveal intriguing collective structures. From the predicted neutron particle-hole character of the low-lying states in these Cr isotopes, ^{62}Cr emerges as a transitional system on the path to the center of the $N = 40$ island of inversion.

DOI: 10.1103/PhysRevC.103.014314

I. INTRODUCTION

On the nuclear chart, an "island of inversion" is formed when a group of nuclei, expected to be spherical in their ground states, based on the normal-order filling of nuclear shells, display collectivity. Among the driving forces forming such regions is the strong nuclear quadrupole-quadrupole interaction, prompting a shape transition in which highly correlated many-particle–many-hole configurations, often called intruder states, become more bound than the spherical ones. The islands of inversion around ^{12}Be ($N = 8$) [1], ^{32}Mg ($N = 20$) [2–4], and ^{42}Si [5,6] ($N = 28$) have revealed the existence of structural changes for neutron-rich systems, such as the breakdown of magic numbers and rapid shape changes among neighboring nuclei. These regions have been invaluable in unraveling the driving forces of shell evolution including, most broadly, a variety of correlation effects and, specifically, the role of monopole interactions due to the various constituents of the NN interaction such as the tensor and central forces [4,6–8]. The newest addition to the group of islands of inversion is centered on ^{64}Cr ($N = 40$) [9], where Cr and Fe isotopes are among the most deformed in the region [10–13] in spite of an originally proposed $N = 40$ harmonic oscillator shell gap [14]. This island, at its boundary, also harbors the noteworthy case of triple shape coexistence in ^{68}Ni [15,16], just four protons north of ^{64}Cr, with such coexistence also reported in the neighboring Ni isotopes [17–19]. A recent prediction extends this island of inversion to $N = 50$ [20], and includes nuclei that will only be reached at next-generation rare-isotope beam facilities.

This prospect of extending the island towards magic neutron number $N = 50$ is based on extrapolations of calculations using the Lenzi-Nowacki-Poves-Sieja (LNPS) shell-model effective interaction and its monopole drifts [9,20]. These have been successful in predicting the energies of the only two excited states, 2_1^+ and (4_1^+) [12], known for the key nucleus ^{64}Cr at the center of the island. While shape coexistence has been prominently displayed by nuclei at the boundary of islands of inversion, for example in ^{34}Si ($N = 20$ island of inversion) [21] and in ^{68}Ni as discussed above, a low-lying, presumably shape-coexisting 0^+ state has also been established in ^{32}Mg [22,23], at the heart of the $N = 20$ island of inversion, as well as in collective ^{44}S [24–26] at $N = 28$. Given the stark similarities between the $N = 20, 28$ and the $N = 40$ islands of inversion, one may also anticipate finding low-lying shape coexistence in the neutron-rich Cr isotopes. Indeed, as discussed in this work, shell-model calculations based on the LNPS effective interaction predict 0_2^+ states near 1400 and 1600 keV in ^{62}Cr and ^{64}Cr, respectively, and collective structures are anticipated to be built on top of these 0_2^+ levels (see also [27] for an earlier theory discussion on collectivity in the Cr isotopes). Putting those predictions to the test is of interest,

*Present address: Lawrence Livermore National Laboratory, Livermore, California 94550, USA.

given that rapidly evolving coexisting collective structures are fingerprints of the transition to the proposed $N = 50$ island of inversion in very neutron-rich territory [20].

While ^{66}Cr is the most neutron-rich Cr isotope with a known 2_1^+ and proposed (4_1^+) level [28], excited states in ^{64}Cr have only been accessed in three experiments prior to the present work: The first γ-ray spectroscopy identifying the 2_1^+ and (4_1^+) states was performed using inelastic scattering off ^{9}Be [12], the $B(E2; 0_1^+ \rightarrow 2_1^+)$ value being subsequently deduced from intermediate-energy Coulomb excitation [13]. The β decay of ^{64}V to ^{64}Cr provided a first precise measurement of the energy of the 2_1^+ state [29]. In ^{62}Cr, only the 2_1^+ and (4_1^+) states are known, from measurements using a variety of approaches [11,12,30–32], including various inelastic scattering probes and β decay. To provide first exploratory γ-ray spectroscopy beyond the (4_1^+) state in ^{62,64}Cr, a measurement was performed with nucleon-removal reactions from several projectiles within a multicomponent rare-isotope beam in order to populate excited states in the two isotopes of interest. The results are discussed in comparison to the shell-model predictions of rich low-lying level schemes for these two isotopes. An outlook is provided on how future experiments may target the interesting coexisting structures emerging from the shell-model description of this region.

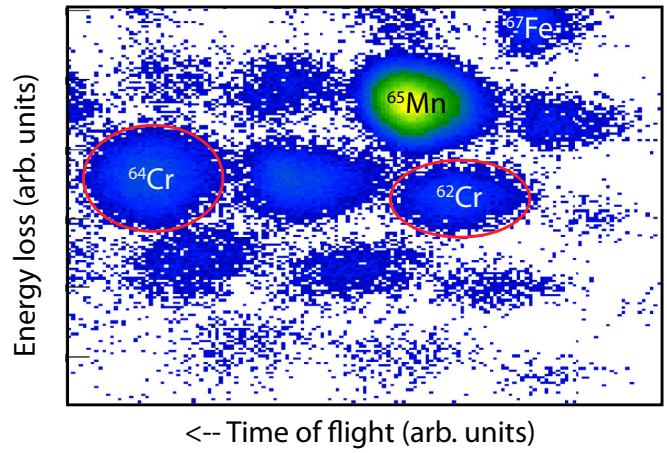

FIG. 1. Example particle-identification spectrum for the reactions induced by ^{65}Mn, energy loss vs time of flight as determined with the S800 ionization chamber and two plastic timing scintillators. The projectile beam leaking in the S800 focal plane and the Cr reaction residues of interest are marked. Also visible is a small amount of ^{67}Fe projectiles together with the associated reaction residues, not impacting the identification of the Cr isotopes. The particle-identification plot only shows particles that registered a γ ray in coincidence.

II. EXPERIMENT

Excited states in ^{64,62}Cr were populated in nucleon-removal reactions induced by ^{65}Mn, ^{66}Fe, and ^{68}Co projectiles at 90–95 MeV/u at NSCL's Coupled Cyclotron Facility [33]. The secondary beam including these projectiles was produced by fragmentation of a 140-MeV/u primary beam of ^{82}Se impinging on a 329-mg/cm^2 ^{9}Be production target, and was separated using a 300-mg/cm^2 Al degrader in the A1900 fragment separator [34]. The momentum acceptance of the separator was set to $\Delta p/p = 2\%$. The beam composition was as follows: 9.5% of ^{65}Mn, 40% of ^{66}Fe, and 46% of ^{68}Co. Weaker beam constituents such as ^{67}Fe, ^{69}Ni, and ^{67}Co were each below 2% in abundance. The 376-mg/cm^2-thick ^{9}Be target was located at the target position of the S800 spectrograph. The projectile-like reaction residues were identified on an event-by-event basis in the S800 focal plane [35] from their energy loss and flight time. For the first half of the experiment, the magnetic rigidity was optimized to center ^{64}Cr produced from ^{65}Mn in the S800 focal plane, while the second half proceeded with this rigidity shifted slightly to move the Cr isotopes of interest produced from ^{66}Fe and ^{68}Co more into the focal-plane acceptance. The particle identification for the reactions induced by ^{65}Mn is shown in Fig. 1. For this purpose, the ^{65}Mn projectiles in the entrance channel were selected through a software gate applied on the time-of-flight difference taken between two plastic timing scintillators located before the target.

The much more abundant and essentially equally intense ^{66}Fe and ^{68}Co projectiles overlapped in time-of-flight difference and, therefore, could not be separated in the incoming beam at $\Delta p/p = 2\%$ momentum acceptance. As a result, the corresponding particle identification spectrum contains ^{64,62}Cr produced from both projectiles in the same gate. Since this experiment was designed as a pure spectroscopy measurement, optimized for the γ-ray yields in the ^{62,64}Cr isotopes, the rigidity change, the associated acceptance losses for each setting and isotope, and the overlapping incoming particle identification for the Fe and Co projectiles were of no concern and cross sections were not determined.

The high-resolution γ-ray detector array GRETINA [36,37], an array of 36-fold segmented high-purity germanium detectors assembled into modules housing four crystals each, was used to detect the prompt γ rays emitted in flight by the reaction residues. The eleven available detector modules were arranged in two rings with four located at 58° and seven at 90° with respect to the beam axis. Online pulse-shape analysis provided the γ-ray interaction points for event-by-event Doppler reconstruction of the γ rays emitted in-flight at about 40% of the speed of light. The interaction point with the maximum energy deposition was assumed to correspond to the first hit for the the γ-ray emission angle determination entering Doppler reconstruction [37]. The momentum vector of projectile-like reaction residues, as ray-traced through the S800 spectrograph, was incorporated into the emission-angle determination. Figures 2 and 3 display the Doppler-reconstructed γ-ray spectra from the different projectile beams for ^{64}Cr and ^{62}Cr, respectively, with nearest-neighbor add-back included [37].

The three dominant peaks in the spectra of ^{64}Cr in Fig. 2 correspond to the two known γ-ray transitions, $2_1^+ \rightarrow 0_1^+$ and $(4_1^+) \rightarrow 2_1^+$, and to a new one at 963 keV. The energies reported for the known transitions agree with previous data [12] and display a common feature of in-beam γ-ray spectroscopy with fast beams: The velocity v/c was chosen such that the 963-keV transition is aligned in the spectra of GRETINA that correspond to forward and 90° angle coverage,

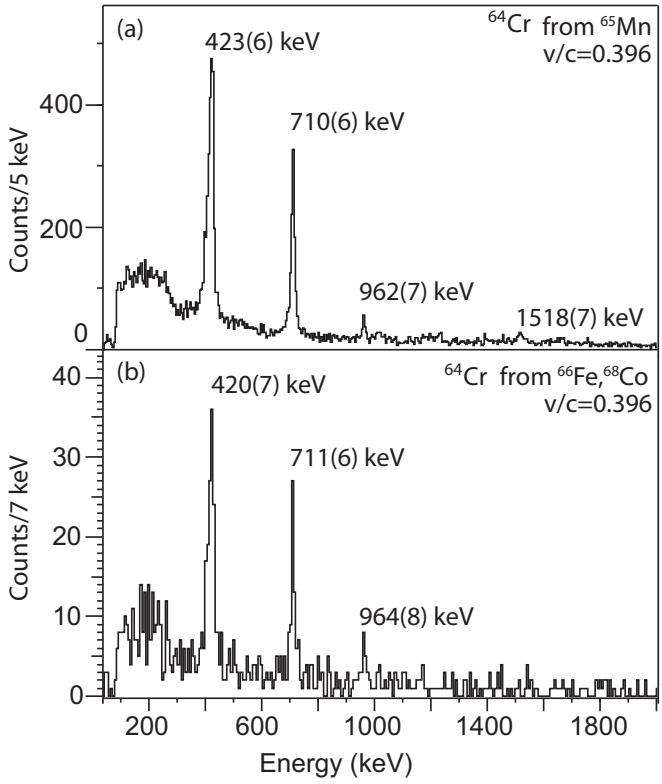

FIG. 2. Doppler-corrected energy spectrum with add-back for ^{64}Cr (a) as produced in one-proton removal from ^{65}Mn projectiles and (b) as produced from ^{66}Fe and ^{68}Co projectiles. The three prominent peaks are labeled by their energy.

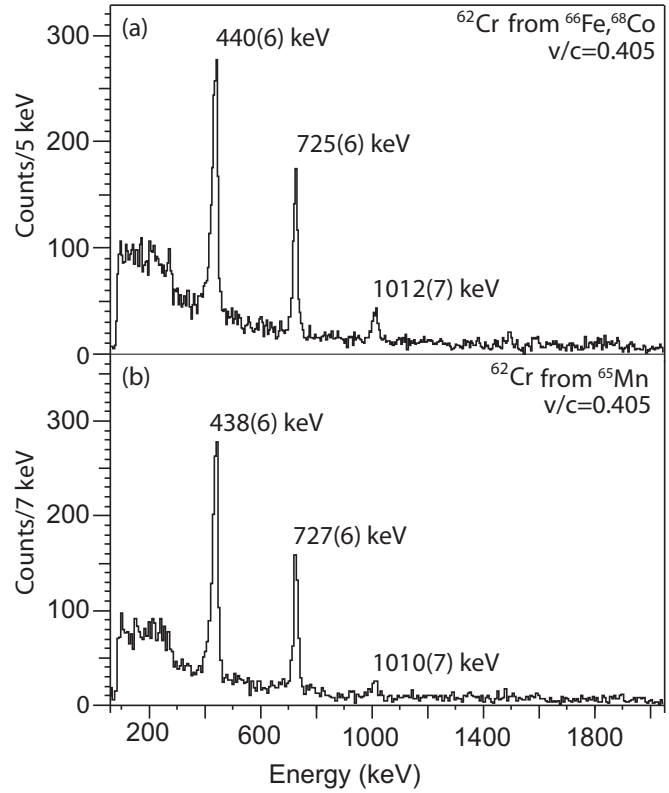

FIG. 3. Doppler-corrected energy spectrum with add-back for ^{62}Cr (a) as produced from ^{66}Fe and ^{68}Co projectiles and (b) as produced from the ^{65}Mn secondary beam. The three prominent peaks are labeled by their energy.

with the assumption that the transition is fast (low picosecond level). However, the $2_1^+ \rightarrow 0_1^+$ transition proceeds with a known mean lifetime of about 177 ps [13], and emission occurs predominantly behind the target, which leads to the forward and 90° GRETINA spectra not lining up at the same v/c value and the energy being Doppler reconstructed to an energy that is too low by a few keV. This is visible through the worsened resolution of the peak and its location at about 422 keV as compared to the precise value from β decay of 430(1) keV. This situation is discussed and confirmed through simulations for the similar case of ^{70}Fe measured within the same experimental scheme [38]. Smaller peaks corresponding to weakly populated transitions are highlighted in Fig. 4(b) and are discussed in more detail below.

Similarly, the dominant peaks in the spectra of ^{62}Cr of Fig. 3 correspond to two known γ rays [39], $2_1^+ \rightarrow 0_1^+$ and $(4_1^+) \rightarrow 2_1^+$, and a new one at 1011 keV. As for ^{64}Cr, the energies agree with previous reports and the 2_1^+ lifetime, which is of order of 100 ps [31,32], leads to an energy that is too low and to a worse resolution when the v/c value is chosen to line up the presumably fast higher-energy transitions [38]. Smaller peaks corresponding to transitions from weakly populated states are highlighted in Fig. 4(a).

Figure 4 expands the sum of the ^{62,64}Cr spectra from the different reaction channels. In addition to the peaks at 1011 and 962 keV in ^{62}Cr and ^{64}Cr, respectively, multiple weaker γ rays appear together with structures that may correspond to one or several transitions. Clear peaks are labeled by their energy and potential peaks or peak-like structures are labeled by energies in parentheses.

III. RESULTS AND DISCUSSION

In the following, we will discuss the obtained results with the help of γ-ray coincidence relationships, high-level arguments based on configurations populated, and comparisons to shell-model calculations using the LNPS effective interaction [9].

Starting with ^{64}Cr, the most statistics are accumulated in the spectrum from the one-proton knockout from ^{65}Mn. According to [39], the ground-state spin-parity of $Z = 25$ ^{65}Mn is $(5/2^-)$. In a schematic picture, the removal of a $f_{5/2}$ proton would populate the ^{64}Cr ground state and, possibly, excited 0^+ states with such a parentage. Removal of one of the $f_{7/2}$ protons will populate $\pi(f_{7/2}^{-1} f_{5/2}^{+1})^{(J^+)}$ configurations, reaching states with spin-parities of $J^+ = 2^+$ to 6^+. This is reminiscent of the situation reported for ^{70}Fe, a collective system also, where such f-shell spectroscopic strength was calculated to be thinly spread across tens of states within the same spin range. This, then, leads to a pandemonium-like [40] scheme where the strong transitions among the lowest-lying states are almost certainly not indicative of the parent level being directly fed through direct reactions. Rather, the feeding occurs

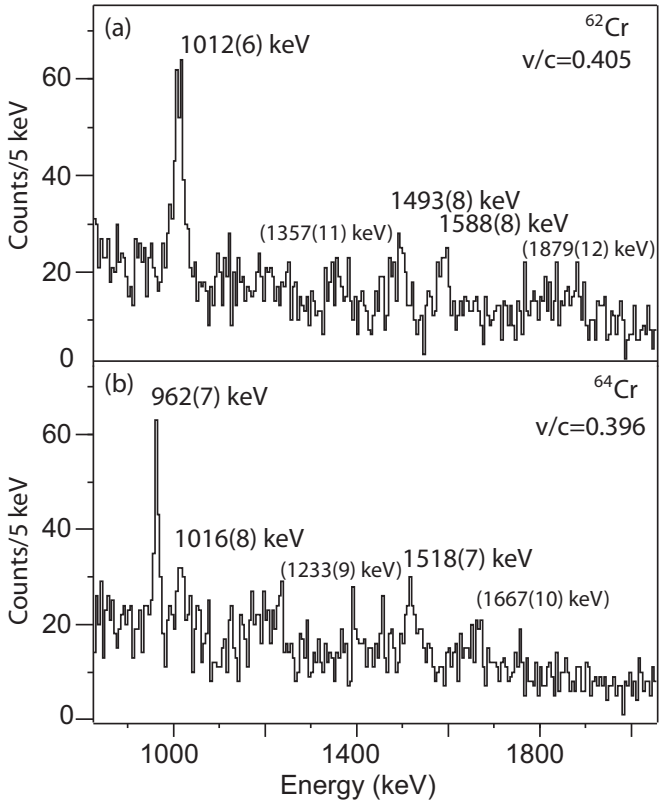

FIG. 4. Expansion of the high-energy part of the summed γ-ray spectra for (a) ^{62}Cr and (b) ^{64}Cr. Clear peaks are labeled by their energy, and suspected peaks or peak-like structures are indicated with an estimated energy in parentheses.

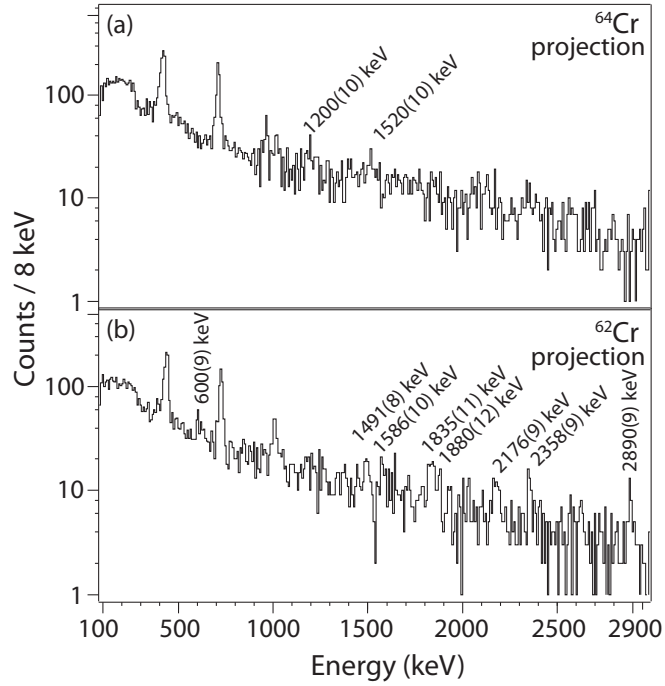

FIG. 5. Projection of the $\gamma\gamma$-coincidence matrices for (a) ^{64}Cr and (b) ^{62}Cr. Higher-energy transitions are labeled by their energy; these largely correspond to the weak peaks marked in Fig. 4, but also comprise potential, very weak transitions above 2 MeV that do not stand out in the singles spectra.

indirectly through many higher-lying levels, each populated weakly [38]. While such a situation essentially prevents a detailed study of the single-proton degree of freedom, perhaps not unexpected for a collective, complex system, it opens the door for γ-ray spectroscopy. For ^{62}Cr produced from ^{65}Mn, while the accessed proton configurations are the same, the loss of neutrons, either as removed by the reaction or by evaporation, will broaden the slate of accessible excited states.

The population of ^{62,64}Cr from ^{66}Fe and ^{68}Co projectiles is complicated by the fact that the present experiment cannot separate these two incoming beams. The two-proton knockout from ^{66}Fe to ^{64}Cr proceeds as a direct reaction with an inclusive cross section of only 0.13(5) mb [41]. In Ref. [41], given the low cross section, statistics were too low for γ-ray spectroscopy, and it was speculated that structural differences between the ^{66}Fe ground state and the bound excited states of ^{64}Cr, driven by complex particle-hole structures involving the neutron $g_{9/2}$ orbital, may lead to a reduced neutron wave function overlap and, thus, to such a small cross section [41]. The accessed proton configurations in the two-proton removal from Fe to Cr will be dominated by $\pi(f_{7/2})^2$ states, leading to 0^+, 2^+, 4^+, and 6^+ levels being populated in a schematic picture, broadened by neutron evaporation or removal for the case of ^{62}Cr. The four to six nucleon removals from ^{68}Co are expected to populate excited states in the Cr isotopes more statistically.

Figure 5 provides the projections of the $\gamma\gamma$-coincidence matrices for ^{64}Cr (a) and ^{62}Cr (b) on a logarithmic scale. This supports the scenario discussed above, of three intense transitions and a multitude of weaker peaks that exhibit $\gamma\gamma$-coincidence relationships, thus likely funneling intensity towards the ground state through the yrast line.

Figure 6 shows the cuts on the $2_1^+ \rightarrow 0_1^+$ (a) and $(4_1^+) \rightarrow 2_1^+$ (b) transitions in the ^{64}Cr $\gamma\gamma$-coincidence matrix (see Fig. 7 for an illustration of the matrix). The software gate on the 423-keV transition returns prominently the $(4_1^+) \rightarrow 2_1^+$ peak at 710 keV. In turn, a gate placed on the 710-keV γ ray displays the expected $2_1^+ \rightarrow 0_1^+$ peak, providing the first proof that these two γ rays, the only ones previously known for ^{64}Cr, are indeed in coincidence as proposed in Ref. [12]. The red line in Fig. 6 indicates the location of the new transition at 963 keV reported here. Within the low statistics, the number of counts agrees with expectations for this γ ray to be in coincidence with both the $2_1^+ \rightarrow 0_1^+$ and $(4_1^+) \rightarrow 2_1^+$ transitions. This is supported by the $\gamma\gamma$ matrix displayed in Fig. 7 where the visible 423-710 and 710-963 keV coincidence events are indicated by red circles.

In ^{62}Cr, the situation is surprisingly different. While—as Fig. 8 indicates—the $2_1^+ \rightarrow 0_1^+$ and $(4_1^+) \rightarrow 2_1^+$ transitions are in mutual coincidence, the new 1011-keV line appears to be in coincidence only with the 2^+ decay and not with the (4_1^+) one. This is also visible in the $\gamma\gamma$-coincidence matrix of Fig. 9 where the coincidences are circled. So, while the spectra of ^{62,64}Cr look very similar, the coincidence relationships seem

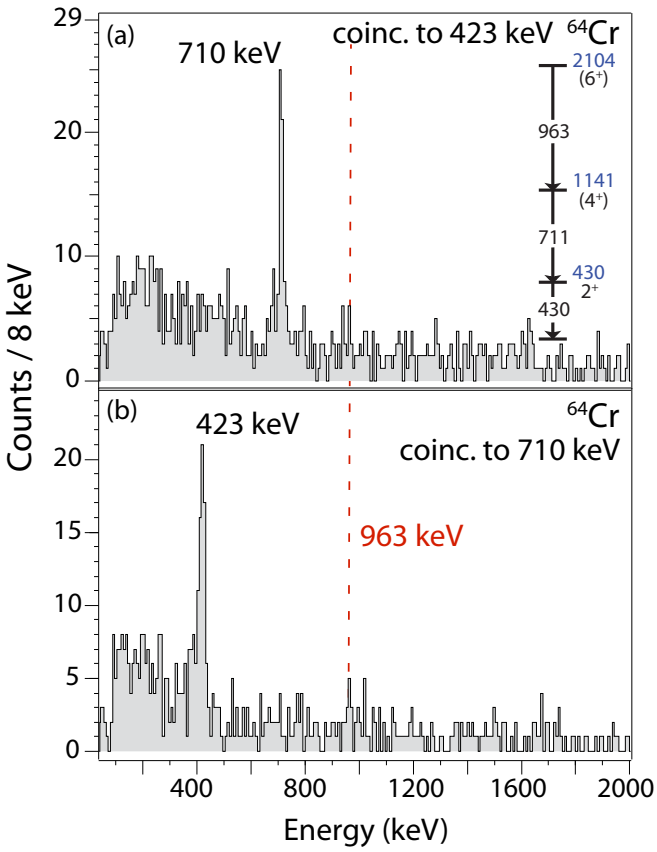

FIG. 6. Coincidence spectra (no background subtraction) for ^{64}Cr, gated on (a) the 423-keV $2_1^+ \rightarrow 0_1^+$ transition and (b) the 710-keV $(4_1^+) \rightarrow 2_1^+$ one. The red dashed line indicates the location where the 963-keV γ ray visible in the singles spectrum and the projection is expected. The inset in the upper panel shows the emerging level scheme from the coincidence relationships with tentative spin assignments. As discussed in the text, the 2_1^+ energy from β decay is used due to lifetime effects in fast-beam spectra.

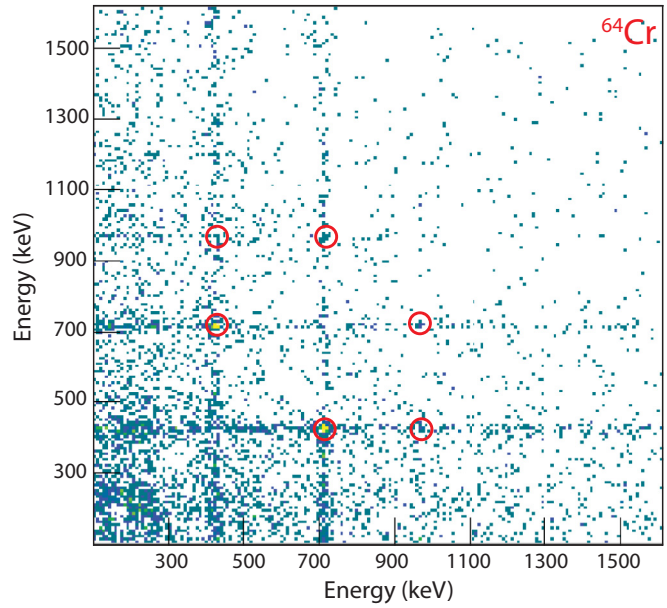

FIG. 7. Coincidence matrix constructed for ^{64}Cr. The $2_1^+ \rightarrow 0_1^+$ and $(4_1^+) \rightarrow 2_1^+$ coincidence is clearly visible and indicated by red circles at the respective 423 and 710 keV energy entries. The coincidence of the newly reported 963-keV line with 710 keV is visible as well and circled.

to reveal a startling difference in the final states accessed through the various reactions.

In view of the low statistics, we briefly quantify the coincidence relationships in support of the conclusions drawn from the spectra and coincidence matrices. For ^{62}Cr, about 1300, 595, and 150 counts at 440, 726, and 1011 keV are visible in the γ-ray singles spectrum, with a GRETINA in-beam full-energy-peak efficiency of 11%, 9%, and 7%, respectively. If the 1011 $\rightarrow$ 726 $\rightarrow$ 440 keV transitions were to form a cascade, for a coincidence gate on the 1011-keV transition, one would expect of the order of 17 and 13 counts in the 440- and 726-keV peaks, respectively, but the background level is too high to discern peaks of such low intensity. However, in turn, if the 1011-keV transition were to feed the lower-lying levels in the cascade, 150 counts $\times$ 11/7 = 235 counts in the 440-keV peak and 150 counts $\times$ 9/7 = 193 counts in the 726-keV line of the singles spectrum would originate from this feeding pattern. Thus, in a coincidence gate on the 440 and 726-keV transitions, one would expect to observe about 17 and 13 counts at 1011 keV, respectively. In Fig. 8, the expected number of 1011-keV counts is indeed realized in the 440-keV coincidence gate, but not in the 726-keV one, strongly supporting our conclusion that the 1011-keV transition feeds the 2_1^+ level but not the 4_1^+ state. For ^{64}Cr, about 2500, 1145, and 95 counts are observed at 423, 710, and 963 keV, respectively. At these energies, GRETINA's full-energy peak efficiency, including the corresponding Lorentz boost, amounts to 11%, 9%, and 8%, respectively. Following the same argumentation outlined above for the ^{62}Cr case, for a coincidence gate placed on the 423- and 710-keV lines, one expects to find about 10 and 8 counts in the 963-keV peak, respectively, and this is in line with observations in the spectra of Fig. 6. Again, gating on the 963-keV transition at the top of the cascade, the expected counts of 10 and 8 at 423 and 710 keV, respectively, are obstructed by the higher background level at lower energy.

It is now interesting to look at the calculated level schemes for these two Cr isotopes. The only shell-model effective interaction available so far that captures well both the onset of collectivity in the neutron-rich Cr and Fe isotopes around $N = 40$ and the presence of coexisting structures in ^{68}Ni is the LNPS one [9]. This is in part attributed to its extensive model space which encompasses the full fp shell for protons and the $0f_{5/2}$, $1p_{3/2}$, $1p_{1/2}$, $0g_{9/2}$, and $1d_{5/2}$ orbitals for neutrons, relative to a ^{48}Ca core [9]. Neutron particle-hole excitations across the $N = 40$ harmonic oscillator shell gap into the $g_{9/2}$ and $d_{5/2}$ orbitals emerge as critical factors in the description of the collective properties. Unlike in the $N = 20$ island of inversion, where neutron two-particle two-hole (2p-2h) excitations from the sd to the fp shell across the $N = 20$ gap are considered to be the main drivers generating collectivity, 4p-4h configurations are thought to dominate in the $N = 40$ island and even 6p-6h excitations are predicted to contribute significantly [9]. This anticipated complexity in the wave

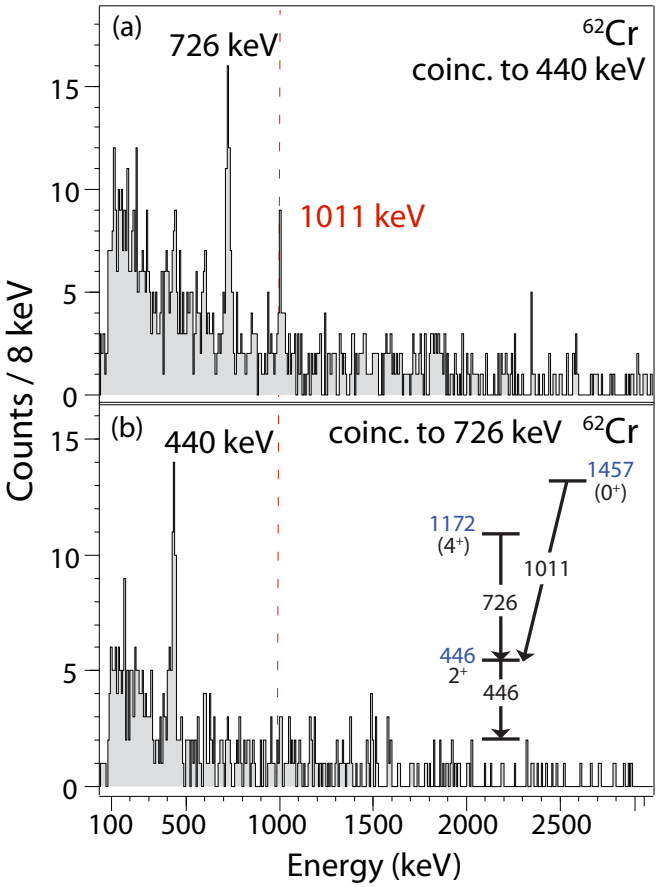

FIG. 8. Coincidence spectra (no background subtraction) for ^{62}Cr, gated on (a) the 440-keV $2_1^+ \rightarrow 0_1^+$ transition and (b) the 726-keV $(4_1^+) \rightarrow 2_1^+$ γ ray. The red dashed line indicates the location where the 1011-keV γ ray, visible in the singles spectrum and the projection, is expected. The inset in the lower panel provides the emerging level scheme from the coincidence relationships with tentative spin assignments. As discussed in the text, the 2_1^+ energy from β decay is used due to lifetime effects in fast-beam data.

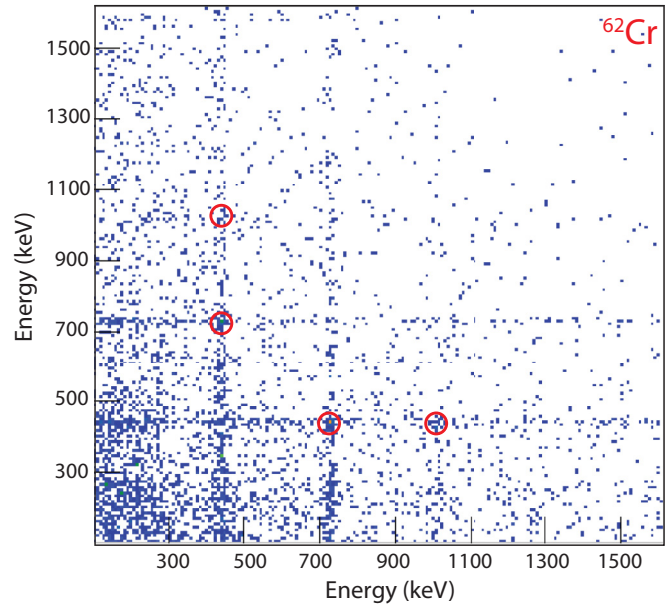

FIG. 9. Coincidence matrix constructed for ^{62}Cr produced from ^{66}Fe and ^{68}Co. The $2_1^+ \rightarrow 0_1^+$ and $(4_1^+) \rightarrow 2_1^+$ coincidence relationship is clearly visible and indicated by red circles at the respective 440 and 726 keV energies. The coincidence of the newly reported 1011-keV line with 440 keV is visible as well and circled.

functions is responsible for the fragmentation of spectroscopic strength calculated for ^{70}Fe in Ref. [38], but one may also expect the large number of particle-hole excitations to add to a diversity in collective structures and shapes.

This rich structure is, indeed, manifested in the calculated level schemes for ^{64,62}Cr as displayed in Figs. 10 and 11. The schemes comprise the lowest-lying positive-parity states and their γ-ray transitions. The arrow thickness is proportional to the associated $B(E2)$ value (with $e_p = 1.31$ and $e_n = 0.46$ as effective charges [42]).

For ^{64}Cr, three distinct quadrupole-collective structures emerge, the (prolate) ground-state sequence, shown here up to the 6^+ state, a band-like structure made up of the 3_1^+, 4_2^+, and 5_1^+ levels built on the 2_2^+ state at 1.8 MeV, and a $\Delta J = 2$ band comprising the 0_2^+ band head and the 2_3^+ and 4_3^+ states. The second structure has some similarity with a gamma band, although the energy ratios of $E(2_2^+)/E(2_1^+) = 3.95$, $E(3_1^+)/E(2_1^+) = 4.6$, and $E(4_2^+)/E(2_1^+) = 5.2$ do not match expectations for a gamma-rigid (30°) or gamma-unstable sequence, with ratios (2.0, 3.0, 5.67) and (2.5, 4.5, 4.5) values, respectively [43]. The third structure could possibly be viewed as a beta band, where the intraband transitions are within 100 keV of $E(2_1^+)$, but as for the gamma-band-like structure, the bandhead is too high in excitation energy. Interestingly, the three computed collective structures are only weakly connected with the $2_3^+ \rightarrow 2_2^+$ transition being the strongest $E2$ link. For completeness, we note that a multiplet of negative-parity states with spin-parities of 3^-, 5^-, and 4^- is predicted at 2.26, 2.33, and 2.42 MeV, respectively. Within the LNPS model space, these states involve 5p-5h neutron excitations from the fp shell to the gd orbitals. Significant population of such neutron configurations would not be anticipated here as reactions predominantly removing protons have been used.

Considering the ^{64}Cr spectra together with the coincidence relationships, and keeping in mind the preferential population of $\pi(f_{7/2}^{-1} f_{5/2}^{+1})^{(J^+)}$ configurations in one-proton removal as well as a pandemonium-like scheme populating the low-lying states indirectly, one may suspect that the 963-keV γ ray corresponds to the $6_1^+ \rightarrow 4_1^+$ transition or a decay of a higher-lying 4^+ level to the 4_1^+ state. In the predicted level scheme (Fig. 11), the 954-keV $6_1^+ \rightarrow 4_1^+$ transition would fit this picture to within 10 keV, in line with the good agreement for the predicted and measured $4_1^+ \rightarrow 2_1^+$ and $2_1^+ \rightarrow 0_1^+$ transitions. Other γ rays in the calculated level scheme feeding the (4_1^+) state within an energy range of ± 250 keV are from the 2_3^+ (971 keV), 3_1^+ (928 keV), and the 4_2^+ (1216 keV) levels. However, all of these states have significant γ-ray branches in addition to the transition of interest (i.e., $2_3^+ \rightarrow 0_2^+$, $4_2^+ \rightarrow 2_1^+$, and $3_1^+ \rightarrow 2_1^+$) and this should have been seen in the data if the state in question had been populated. These

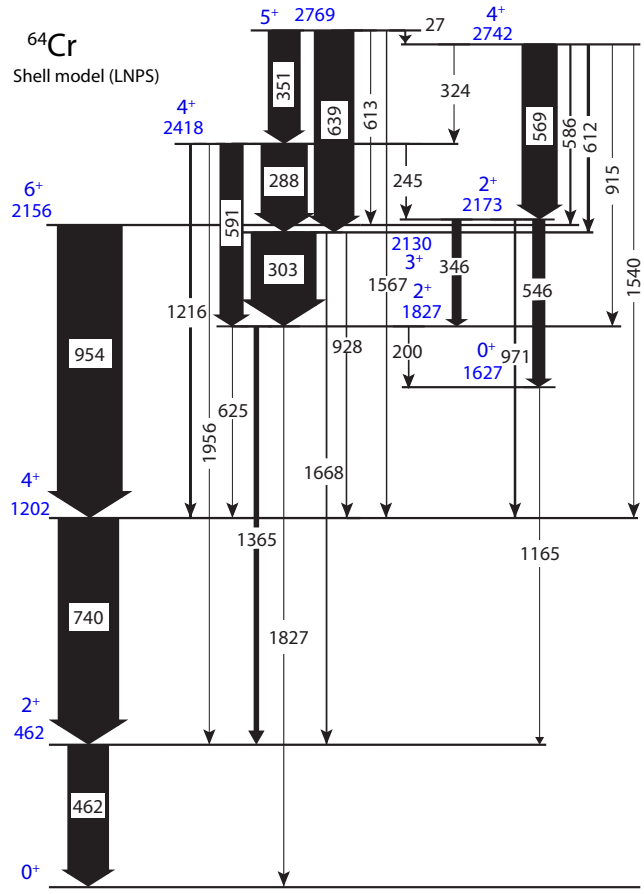

FIG. 10. Level scheme as predicted by shell-model calculations with the LNPS effective interaction for ^{64}Cr. The arrow thickness indicates the magnitude of the $B(E2)$ quadrupole transition strength. A number of collective structures are visible. Only transitions with a predicted transition strength of the order of 1 e^2fm^4 and larger are shown.

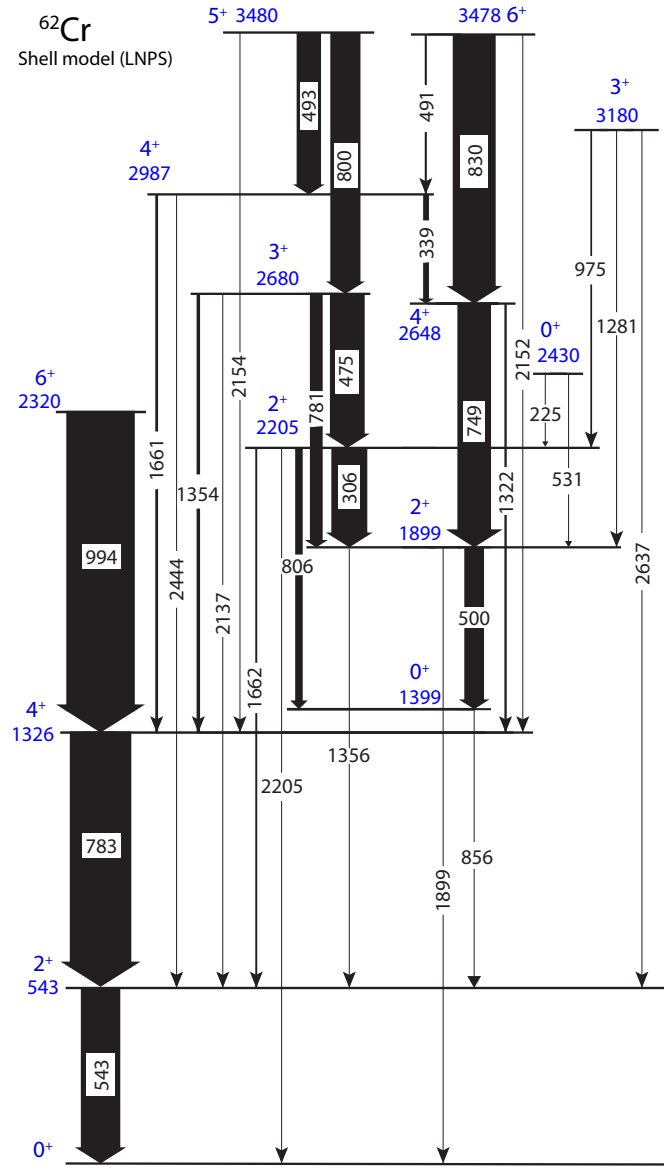

FIG. 11. Level scheme as predicted by shell-model calculations with the LNPS effective interaction for ^{62}Cr. The arrow thickness indicates the magnitude of the $B(E2)$ quadrupole transition strength. A number of collective structures are visible. Only transitions with a predicted transition strength of the order of 1 e^2fm^4 and larger are shown.

considerations make the 6_1^+ assignment most plausible. Note that, if many of the states included in the level scheme of Fig. 10 were populated weakly in the reactions, the multitude of low-intensity peaks visible in the projection of the coincidence matrix (Fig. 5) would be accounted for together with the strong transitions from the 4_1^+ and 2_1^+ states which are predicted to be fed from essentially all higher-lying levels.

In ^{62}Cr, the shell-model calculations again point to three recognizable quadrupole collective structures, but these are now more strongly linked through the 2_2^+ state. In ^{64}Cr, the gamma-like and beta-like bands include the 2_2^+ and 2_3^+ states, respectively, while in ^{62}Cr, the 2_2^+ state is the head of the gamma-like band structure and the 2^+ level of a $\Delta J = 2$ beta-band-like sequence on top of the 0_2^+ state. However, as in ^{64}Cr, there are no strong $E2$ links predicted from either structure to the ground-state band. Again, many of the computed transition energies are close to the weak peaks observed in Fig. 5 and support a pandemonium-like feeding scheme as conjectured already for ^{70}Fe [38].

For ^{62}Cr, given the coincidence spectra and matrix shown in Figs. 8 and 9, the 1011-keV γ ray appears to populate the 2_1^+ rather than the 4_1^+ state. From the calculated level scheme, in such a scenario, the transitions closest in energy to the experiment would be the 856-keV decay of the 0_2^+ state and the 1356-keV one from the 2_2^+ level. Using the shell-model $B(E2; 0_2^+ \rightarrow 2_1^+)$ value together with the measured transition energy of 1011 keV yields a mean lifetime of about 90 ps for the 0_2^+ state which is long and may be the reason for the apparent poorer resolution observed for the 1011-keV ^{62}Cr transition when compared to the 963-keV one in ^{64}Cr (see Fig. 4). More statistics and the precise energy from, e.g., β decay would be needed to quantify a possible lifetime effect. The larger width of the peak could also be due to the presence

of a doublet, for example, of the $6_1^+ \rightarrow 4_1^+$ transition and the $0_2^+ \rightarrow 2_1^+$ one, with the latter being dominant, thereby explaining the measured coincidence relationships and restoring consistency with the observations for neighboring ^{64}Cr, where a candidate for the 6_1^+ state was identified close to the shell-model prediction.

From the shell-model wave functions, the collective states in ^{64}Cr have a dominant neutron 4p-4h character with, on average, three neutron holes in the $f_{5/2}$ orbital and one in the $p_{1/2}$ state and four neutrons excited across $N = 40$ into the *gd* orbitals. The proton configurations are based on one-proton excitations from the $f_{7/2}$ orbital into the $p_{3/2}$ or $f_{5/2}$ ones and, to a lesser extent, into the $p_{1/2}$ state.

While the calculated proton configurations for the states in ^{62}Cr and ^{64}Cr are similar, the neutron particle-hole content for the different collective structures in ^{62}Cr indicates some variation. The ground-state band has a 4p-6h neutron structure with four holes in the $f_{5/2}$ orbital and the two other in the $p_{1/2}$ one and six neutrons excited across $N = 40$ into the *gd* orbitals. The yrare states and the 3_1^+ and 5_1^+ levels are of predominant 2p-4h neutron character, where three of the holes are in the $f_{5/2}$ orbital and the fourth is in the $p_{1/2}$ state, but only two neutrons excited into the *gd* orbitals. The 0_2^+ state is calculated to have a 22% probability of a normal-order 0p-2h neutron configuration with both holes in the $f_{5/2}$ orbital. The 0_3^+ and 2_3^+ levels which both only have very weak $E2$ links to the other structures carry 34% and 7% of this normal-order neutron 0p-2h content. The 3_2^+ state is similarly weakly linked via $E2$ transitions and is computed to be associated with a mixture of neutron 2p-4h and 4p-6h configurations.

From the shell-model configurations above, a picture emerges where ^{64}Cr, with the highest degree of collectivity, has—across all computed band-like structures—predominantly four neutrons occupying orbitals beyond the $N = 40$ subshell gap. In contrast, for ^{62}Cr, the higher-excited collective structures have fewer neutrons occupying the *gd* orbitals, and levels with configurations associated with normal order coexist at roughly the same excitation energy. This transitional character makes ^{62}Cr a critical nucleus for benchmarking our understanding of the onset of the neutron particle-hole configurations defining the $N = 40$ island of inversion.

It is interesting to speculate how one could possibly study the various collective structures in these neutron-rich Cr isotopes. While projectile Coulomb excitation measurements near the Coulomb barrier will undoubtedly enable the determination of the transition strengths in the ground-state bands of ^{62,64}Cr, the other collective structures are calculated to be rather disconnected with only weak linking $E2$ transitions such that cross sections for multistep excitations will be small. Complex (e.g., deep-inelastic) reactions are known to reach higher-spin states and might populate the anticipated collective structures. In Ref. [44], complex ^{48}Ca + ^{26}Mg reactions at energies roughly 200% above the Coulomb barrier resulted in the production of a large number of isotopes with $Z =$ 25–28 comprising both proton- and neutron-rich products. It is possible that reactions of the same type such as ^{48}Ca + ^{22}Ne might reach the neutron-rich Cr isotopes. Alternatively, fusion or few-neutron transfer reactions with a radioactive projectile might become possible, once the next-generation exotic beam facilities are operational.

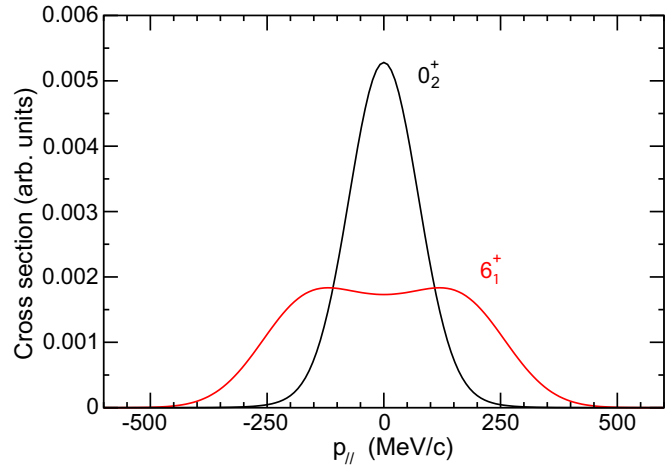

FIG. 12. Calculated longitudinal momentum distributions for the two-proton knockout reaction ^{9}Be(^{64}Fe, ^{62}Cr)X at 80 MeV/u. The shapes of the exclusive momentum distributions clearly differentiate between those for the 0_2^+ and 6_1^+ levels, offering the opportunity to assign a spin value to the state deexcited through the 1011-keV transition in ^{62}Cr in a future measurement. The calculations are meant to illustrate the distinctive shape and are normalized to one unit of cross section. The calculated exclusive cross sections are $\sigma(0_2^+) = 0.09$ and $\sigma(6_1^+) = 0.021$ mb, respectively, totaling 38% of the cross section to the ground state.

To clarify the nature of the 1011-keV transition in ^{62}Cr, we propose a two-proton knockout reaction, ^{9}Be(^{64}Fe, ^{62}Cr$+\gamma$)X, with final-state exclusive measurements of the longitudinal momentum distributions of ^{62}Cr. As already demonstrated in Refs. [25,45,46], the shape of the knockout residue's parallel momentum distribution depends strongly on the total angular momentum of the two removed nucleons, and, at a more detailed level, on the components of the total orbital angular momentum [47,48]. By combining an eikonal model of the reaction dynamics [49] and the LNPS shell-model calculations of the two-proton amplitudes connecting the ^{64}Fe ground state and the ^{62}Cr final states, the cross sections for two-proton knockout from the ^{64}Fe ground state to the 0_2^+ and 6_1^+ states of ^{62}Cr and associated parallel momentum distributions were calculated. As demonstrated in Fig. 12, this would allow for an unambiguous discrimination of the scenarios discussed above; i.e., (i) whether the 1011-keV γ ray originates from the 0_2^+ state of ^{62}Cr, raising the question as to why the 6^+ state was not observed here, or (ii) that it is a doublet comprising the $0_2^+ \rightarrow 2_1^+$ and $6_1^+ \rightarrow 4_1^+$ transitions. An estimated $\sigma(6_1^+)/\sigma(0_2^+) = 23\%$ broad contribution to the dominant, narrow 0^+ distribution appears to be easily identifiable. Regarding the impact of unobserved feeding, potentially missed high-spin feeders of the 6_1^+ state would preserve the broad shape of the momentum distribution, while indirect feeding to the 0_2^+ level would most probably be due to decay branches from higher-lying 2^+ states, only marginally broadening the observed 0^+ momentum distribution, in particular as compared to that of the 6^+ state. We note that

two-nucleon knockout reactions are typically rather selective, reducing the expected level density, and that low-lying 0^+ states have been notoriously hard to find [21–24], in part because their population appears to be selective with only minor indirect feeding in typical reactions.

IV. SUMMARY

We have performed exploratory γ-ray spectroscopy beyond the (4_1^+) states in ^{62,64}Cr, using nucleon-removal reactions from several projectiles within a multicomponent rare-isotope beam to populate excited states in the two isotopes of interest. A candidate for the 6_1^+ state in ^{64}Cr is proposed. The situation is more complex in ^{62}Cr, with the possibility that a 0_2^+ level might have been observed. The results are discussed in comparison to the LNPS shell-model predictions of rich low-lying ^{62,64}Cr level schemes. Interesting collective structures are predicted within the shell model for both Cr isotopes, with their particle-hole character revealing ^{62}Cr to be an important transitional system on the path to the collective center of the $N = 40$ island of inversion. An outlook is provided on how future experiments could target these coexisting structures emerging from the shell-model description of this region.

ACKNOWLEDGMENTS

This work was supported by the U.S. National Science Foundation (NSF) under Grant No. PHY-1565546, by the DOE National Nuclear Security Administration through the Nuclear Science and Security Consortium, under Award No. DE-NA0003180, and by the U.S. Department of Energy, Office of Science, Office of Nuclear Physics, under Grants No. DE-SC0020451 (MSU), No. DE-FG02-97ER41041 (UNC), and No. DE-FG02-97ER41033 (TUNL). GRETINA was funded by the DOE, Office of Science. Operation of the array at NSCL was supported by the DOE under Grant No. DE-SC0019034. J.A.T. acknowledges support from the Science and Technology Facilities Council (U.K.) Grant No. ST/L005743/1. A.P. acknowledges the support of the Ministerio de Ciencia, Innovacion y Universidades (Spain), Severo Ochoa Programme SEV-2016-0597 and Grant No. PGC-2018-94583. We acknowledge discussions with H. L. Crawford and P. Fallon.

[1] I. Talmi and I. Unna, Phys. Rev. Lett. **4**, 469 (1960).
[2] C. Thibault, R. Klapisch, C. Rigaud, A. M. Poskanzer, R. Prieels, L. Lessard, and W. Reisdorf, Phys. Rev. C **12**, 644 (1975).
[3] A. Poves and J. Retamosa, Phys. Lett. B **184**, 311 (1987).
[4] E. K. Warburton, J. A. Becker, and B. A. Brown, Phys. Rev. C **41**, 1147 (1990).
[5] B. Bastin, S. Grevy, D. Sohler, O. Sorlin, Zs. Dombradi, N. L. Achouri, J. C. Angelique, F. Azaiez, D. Baiborodin, R. Borcea, C. Bourgeois, A. Buta, A. Bürger, R. Chapman, J. C. Dalouzy, Z. Dlouhy, A. Drouard, Z. Elekes, S. Franchoo, S. Iacob *et al.*, Phys. Rev. Lett. **99**, 022503 (2007).
[6] E. Caurier, F. Nowacki, and A. Poves, Phys. Rev. C **90**, 014302 (2014).
[7] B. A. Brown, Physics **3**, 104 (2010).
[8] T. Otsuka, A. Gade, O. Sorlin, T. Suzuki, and Y. Utsuno, Rev. Mod. Phys. **92**, 015002 (2020).
[9] S. M. Lenzi, F. Nowacki, A. Poves, and K. Sieja, Phys. Rev. C **82**, 054301 (2010).
[10] M. Hannawald, T. Kautzsch, A. Wöhr, W. B. Walters, K.-L. Kratz, V. N. Fedoseyev, V. I. Mishin, W. Böhmer, B. Pfeiffer, V. Sebastian, Y. Jading, U. Köster, J. Lettry, H. L. Ravn, and the ISOLDE Collaboration, Phys. Rev. Lett. **82**, 1391 (1999).
[11] O. Sorlin, C. Donzaud, F. Nowacki, J. C. Angélique, F. Azaiez, C. Bourgeois, V. Chiste, Z. Dlouhy, S. Grévy, D. Guillemaud-Mueller, F. Ibrahim, K.-L Kratz, M. Lewitowicz, S. M. Lukyanov, J. Mrasek, Yu.-E. Penionzhkevich, F. de Oliveira Santos, B. Pfeiffer, F. Pougheon, A. Poves, M. G. Saint-Laurent, and M. Stanoiu, Eur. Phys. J. A **16**, 55 (2003).
[12] A. Gade, R. V. F. Janssens, T. Baugher, D. Bazin, B. A. Brown, M. P. Carpenter, C. J. Chiara, A. N. Deacon, S. J. Freeman, G. F. Grinyer, C. R. Hoffman, B. P. Kay, F. G. Kondev, T. Lauritsen, S. McDaniel, K. Meierbachtol, A. Ratkiewicz, S. R. Stroberg, K. A. Walsh, D. Weisshaar, R. Winkler, and S. Zhu, Phys. Rev. C **81**, 051304(R) (2010).
[13] H. L. Crawford, R. M. Clark, P. Fallon, A. O. Macchiavelli, T. Baugher, D. Bazin, C. W. Beausang, J. S. Berryman, D. L. Bleuel, C. M. Campbell, M. Cromaz, G. de Angelis, A. Gade, R. O. Hughes, I. Y. Lee, S. M. Lenzi, F. Nowacki, S. Paschalis, M. Petri, A. Poves, A. Ratkiewicz, T. J. Ross, E. Sahin, D. Weisshaar, K. Wimmer, and R. Winkler, Phys. Rev. Lett. **110**, 242701 (2013).
[14] M. Bernas, Ph. Dessagne, M. Langevin, J. Payet, F. Pougheon, and P. Roussel, Phys. Lett. B **113**, 279 (1982).
[15] S. Suchyta, S. N. Liddick, Y. Tsunoda, T. Otsuka, M. B. Bennett, A. Chemey, M. Honma, N. Larson, C. J. Prokop, S. J. Quinn, N. Shimizu, A. Simon, A. Spyrou, V. Tripathi, Y. Utsuno, and J. M. VonMoss, Phys. Rev. C **89**, 021301(R) (2014).
[16] Y. Tsunoda, T. Otsuka, N. Shimizu, M. Honma, and Y. Utsuno, Phys. Rev. C **89**, 031301(R) (2014).
[17] B. P. Crider, C. J. Prokop, S. N. Liddick, M. Al-Shudifat, A. D. Ayangeakaa, M. P. Carpenter, J. J. Carroll, J. Chen, C. J. Chiara, H. M. David, A. C. Dombos, S. Go, R. Grzywaczc, J. Harker, R. V. F. Janssens, N. Larson, T. Lauritsen, R. Lewis, S. J. Quinn, F. Recchia, A. Spyrou, S. Suchyta, W. B. Walters, and S. Zhu, Phys. Lett. B **763**, 108 (2016).
[18] S. Leoni, B. Fornal, N. Mărginean, M. Sferrazza, Y. Tsunoda, T. Otsuka, G. Bocchi, F. C. L. Crespi, A. Bracco, S. Aydin, M. Boromiza, D. Bucurescu, N. Cieplicka-Oryńczak, C. Costache, S. Călinescu, N. Florea, D. G. Ghiţă, T. Glodariu, A. Ionescu, Ł. W. Iskra *et al.*, Phys. Rev. Lett. **118**, 162502 (2017).
[19] N. Mărginean, D. Little, Y. Tsunoda, S. Leoni, R. V. F. Janssens, B. Fornal, T. Otsuka, C. Michelagnoli, L. Stan, F. C. L. Crespi, C. Costache, R. Lica, M. Sferrazza, A. Turturica, A. D. Ayangeakaa, K. Auranen, M. Barani, P. C. Bender, S. Bottoni, M. Boromiza, A. Bracco, S. Calinescu, C. M. Campbell,

M. P. Carpenter, P. Chowdhury, M. Ciemala *et al.*, Phys. Rev. Lett. **125**, 102502 (2020).
[20] F. Nowacki, A. Poves, E. Caurier, and B. Bounthong, Phys. Rev. Lett. **117**, 272501 (2016).
[21] F. Rotaru, F. Negoita, S. Grevy, J. Mrazek, S. Lukyanov, F. Nowacki, A. Poves, O. Sorlin, C. Borcea, R. Borcea, A. Buta, L. Caceres, S. Calinescu, R. Chevrier, Zs. Dombradi, J. M. Daugas, D. Lebhertz, Y. Penionzhkevich, C. Petrone, D. Sohler, M. Stanoiu, and J. C. Thomas, Phys. Rev. Lett. **109**, 092503 (2012).
[22] K. Wimmer, T. Kröll, R. Krücken, V. Bildstein, R. Gernhäuser, B. Bastin, N. Bree, J. Diriken, P. Van Duppen, M. Huyse, N. Patronis, P. Vermaelen, D. Voulot, J. Van de Walle, F. Wenander, L. M. Fraile, R. Chapman, B. Hadinia, R. Orlandi, J. F. Smith, R. Lutter, P. G. Thirolf *et al.*, Phys. Rev. Lett. **105**, 252501 (2010).
[23] R. Elder, H. Iwasaki, J. Ash, D. Bazin, P. C. Bender, T. Braunroth, B. A. Brown, C. M. Campbell, H. L. Crawford, B. Elman, A. Gade, M. Grinder, N. Kobayashi, B. Longfellow, A. O. Macchiavelli, T. Mijatović, J. Pereira, A. Revel, D. Rhodes, J. A. Tostevin, and D. Weisshaar, Phys. Rev. C **100**, 041301(R) (2019).
[24] C. Force, S. Grévy, L. Gaudefroy, O. Sorlin, L. Cáceres, F. Rotaru, J. Mrazek, N. L. Achouri, J. C. Angélique, F. Azaiez, B. Bastin, R. Borcea, A. Buta, J. M. Daugas, Z. Dlouhy, Zs. Dombrádi, F. De Oliveira, F. Negoita, Y. Penionzhkevich, M. G. Saint-Laurent, D. Sohler, M. Stanoiu, I. Stefan, C. Stodel, and F. Nowacki, Phys. Rev. Lett. **105**, 102501 (2010).
[25] D. Santiago-Gonzalez, I. Wiedenhöver, V. Abramkina, M. L. Avila, T. Baugher, D. Bazin, B. A. Brown, P. D. Cottle, A. Gade, T. Glasmacher, K. W. Kemper, S. McDaniel, A. Rojas, A. Ratkiewicz, R. Meharchand, E. C. Simpson, J. A. Tostevin, A. Volya, and D. Weisshaar, Phys. Rev. C **83**, 061305(R) (2011).
[26] J. J. Parker IV, I. Wiedenhöver, P. D. Cottle, J. Baker, D. McPherson, M. A. Riley, D. Santiago-Gonzalez, A. Volya, V. M. Bader, T. Baugher, D. Bazin, A. Gade, T. Ginter, H. Iwasaki, C. Loelius, C. Morse, F. Recchia, D. Smalley, S. R. Stroberg, K. Whitmore, D. Weisshaar, A. Lemasson, H. L. Crawford, A. O. Macchiavelli, and K. Wimmer, Phys. Rev. Lett. **118**, 052501 (2017).
[27] J. Kotila and S. M. Lenzi, Phys. Rev. C **89**, 064304 (2014).
[28] C. Santamaria, C. Louchart, A. Obertelli, V. Werner, P. Doornenbal, F. Nowacki, G. Authelet, H. Baba, D. Calvet, F. Chateau, A. Corsi, A. Delbart, J.-M. Gheller, A. Gillibert, T. Isobe, V. Lapoux, M. Matsushita, S. Momiyama, T. Motobayashi, M. Niikura, H. Otsu *et al.*, Phys. Rev. Lett. **115**, 192501 (2015).
[29] S. Suchyta, S. N. Liddick, C. J. Chiara, W. B. Walters, M. P. Carpenter, H. L. Crawford, G. F. Grinyer, G. Gürdal, A. Klose, E. A. McCutchan, J. Pereira, and S. Zhu, Phys. Rev. C **89**, 067303 (2014).
[30] N. Aoi, E. Takeshita, H. Suzuki, S. Takeuchi, S. Ota, H. Baba, S. Bishop, T. Fukui, Y. Hashimoto, H. J. Ong, E. Ideguchi, K. Ieki, N. Imai, M. Ishihara, H. Iwasaki, S. Kanno, Y. Kondo, T. Kubo, K. Kurita, K. Kusaka, T. Minemura, T. Motobayashi, T. Nakabayashi *et al.*, Phys. Rev. Lett. **102**, 012502 (2009).
[31] T. Baugher, A. Gade, R. V. F. Janssens, S. M. Lenzi, D. Bazin, B. A. Brown, M. P. Carpenter, A. N. Deacon, S. J. Freeman, T. Glasmacher, G. F. Grinyer, F. G. Kondev, S. McDaniel, A. Poves, A. Ratkiewicz, E. A. McCutchan, D. K. Sharp, I. Stefanescu, K. A. Walsh, D. Weisshaar, and S. Zhu, Phys. Rev. C **86**, 011305(R) (2012); **86**, 049902(E) (2012).
[32] T. Braunroth, A. Dewald, H. Iwasaki, S. M. Lenzi, M. Albers, V. M. Bader, T. Baugher, T. Baumann, D. Bazin, J. S. Berryman, C. Fransen, A. Gade, T. Ginter, A. Gottardo, M. Hackstein, J. Jolie, A. Lemasson, J. Litzinger, S. Lunardi, T. Marchi, V. Modamio *et al.*, Phys. Rev. C **92**, 034306 (2015).
[33] A. Gade and B. M. Sherrill, Phys. Scr. **91**, 053003 (2016).
[34] D. J. Morrissey, B. M. Sherrill, M. Steiner, A. Stolz, and I. Wiedenhöver, Nucl. Instrum. Methods Phys. Res. B **204**, 90 (2003).
[35] D. Bazin, J. A. Caggiano, B. M. Sherrill, J. Yurkon, and A. Zeller, Nucl. Instrum. Methods Phys. Res. B **204**, 629 (2003).
[36] S. Paschalis *et al.*, Nucl. Instrum. Methods Phys. Res., Sect. A **709**, 44 (2013).
[37] D. Weisshaar, D. Bazin, P. C. Bender, C. M. Campbell, F. Recchia, V. Bader, T. Baugher, J. Belarge, M. P. Carpenter, H. L. Crawford, M. Cromaz, B. Elman, P. Fallon, A. Forney, A. Gade, J. Harker, N. Kobayashi, C. Langer, T. Lauritsen, I. Y. Lee, A. Lemasson, B. Longfellow *et al.*, Nuclear Instrum. Methods Phys. Res., Sect. A **847**, 187 (2017).
[38] A. Gade, R. V. F. Janssens, J. A. Tostevin, D. Bazin, J. Belarge, P. C. Bender, S. Bottoni, M. P. Carpenter, B. Elman, S. J. Freeman, T. Lauritsen, S. M. Lenzi, B. Longfellow, E. Lunderberg, A. Poves, L. A. Riley, D. K. Sharp, D. Weisshaar, and S. Zhu, Phys. Rev. C **99**, 011301(R) (2019).
[39] Retrieved from the National Nuclear Data Center (NNDC) ENSDF database, 06/2020, https://www.nndc.bnl.gov/index.jsp.
[40] J. C. Hardy, L. C. Carraz, B. Jonson, and P. G. Hansen, Phys. Lett. **71**, 307 (1977).
[41] P. Adrich, A. M. Amthor, D. Bazin, M. D. Bowen, B. A. Brown, C. M. Campbell, J. M. Cook, A. Gade, D. Galaviz, T. Glasmacher, S. McDaniel, D. Miller, A. Obertelli, Y. Shimbara, K. P. Siwek, J. A. Tostevin, and D. Weisshaar, Phys. Rev. C **77**, 054306 (2008).
[42] M. Dufour and A. P. Zuker, Phys. Rev. C **54**, 1641 (1996).
[43] R. F. Casten, *Nuclear Structure from a Simple Perspective* (Oxford University Press, New York, 2000).
[44] M. Albers, S. Zhu, R. V. F. Janssens, J. Gellanki, I. Ragnarsson, M. Alcorta, T. Baugher, P. F. Bertone, M. P. Carpenter, C. J. Chiara, P. Chowdhury, A. N. Deacon, A. Gade, B. DiGiovine, C. R. Hoffman, F. G. Kondev, T. Lauritsen, C. J. Lister, E. A. McCutchan, D. S. Moerland, C. Nair, A. M. Rogers, and D. Seweryniak, Phys. Rev. C **88**, 054314 (2013).
[45] E. C. Simpson, J. A. Tostevin, D. Bazin, B. A. Brown, and A. Gade, Phys. Rev. Lett. **102**, 132502 (2009).
[46] E. C. Simpson, J. A. Tostevin, D. Bazin, and A. Gade, Phys. Rev. C **79**, 064621 (2009).
[47] E. C. Simpson and J. A. Tostevin, Phys. Rev. C **82**, 044616 (2010).
[48] B. Longfellow, A. Gade, J. A. Tostevin, E. C. Simpson, B. A. Brown, A. Magilligan, D. Bazin, P. C. Bender, M. Bowry, B. Elman, E. Lunderberg, D. Rhodes, M. Spieker, D. Weisshaar, and S. J. Williams, Phys. Rev. C **101**, 031303(R) (2020).
[49] J. A. Tostevin and B. A. Brown, Phys. Rev. C **74**, 064604 (2006).